

ARTICLE TYPE

A Volume-agglomeration multirate time advancing for high Reynolds number flow simulation

Emmanuelle Itam¹ | Stephen Wornom² | Bruno Koobus¹ | Alain Dervieux^{*2,3}

¹IMAG, Org Name, State name,
Country name

²Lemma, Lemma, State name,
Country name

³Ecuador, UCA/INRIA, State name,
Country name

Correspondence

*Corresponding author name, This is
sample corresponding address. Email:
authorone@gmail.com

Present Address

This is sample for present address text
this is sample for present address text

Summary

A frequent configuration in computational fluid mechanics combines an explicit time advancing scheme for accuracy purposes and a computational grid with a very small portion of much smaller elements than in the remaining mesh. Two examples of such situations are the travel of a discontinuity followed by a moving mesh, and the large eddy simulation of high Reynolds number flows around bluff bodies where together very thin boundary layers and vortices of much more important size need to be captured. For such configurations, explicit time advancing schemes with global time stepping are very costly. In order to reduce this problem, the multirate time stepping approach represents an interesting improvement. The objective of such schemes, which allow to use *different time steps* in the computational domain, is to avoid penalizing the computational cost of the time advancement of unsteady solutions which would become large due to the use of small global time steps imposed by the smallest elements such as those constituting the boundary layers. In the present work, a new multirate scheme based on control volume agglomeration is proposed for the solution of the compressible Navier-Stokes equations possibly equipped with turbulence models. The method relies on a prediction step where large time steps are performed with an evaluation of the fluxes on macro-cells for the smaller elements for stability purpose, and on a correction step in which small time steps are employed only for the smaller elements. The accuracy and efficiency of the proposed method are evaluated on several benchmark flows: the problem of a moving contact discontinuity (inviscid flow), the computation with a hybrid turbulence model of flows around bluff bodies like a tandem cylinders at Reynolds number 1.66×10^5 , a circular cylinder at Reynolds number 8.4×10^6 , and a flow around a space probe model at Reynolds number 10^6 .

KEYWORDS:

computational fluid dynamics, multirate time advancing, explicit scheme, volume agglomeration, unstructured grid, hybrid turbulence model

1 INTRODUCTION

A frequent configuration in CFD calculations combines an explicit time advancing scheme for accuracy purpose and a computational grid with a very small portion of much smaller elements than in the remaining mesh. Two typical examples are the following:

A first example is the hybrid RANS/LES simulation of high Reynolds number flows around bluff bodies. In that case, very thin boundary layers need be addressed with extremely small cells. When applying explicit time advancing, the computation is penalized by the very small time-step to be applied (CFL number of order 1). But this is not the only interesting region of the computational domain. An important part of the meshing effort is devoted to large regions of medium cell size in which the motion of vortices need be accurately captured. For these vortices, the efficient and accurate time-step is of order of the ratio of local mesh size by vortex velocity. We can apply an implicit scheme with such a time-step, which would produce a local CFL of order 1 for the vortices advection and a local CFL of order hundreds for the boundary layer. However, this can have several disadvantages. First, of course, this standpoint neglects completely a possible need of unsteady accuracy in the small-cell region. Second, considering the need of accuracy for vortices motion on medium cells, highly accurate explicit schemes are easily assembled. This includes the TVD third-order ones, and the standard RK4. In contrast, high-order implicit schemes are complex and cpu consuming. More simple implicit schemes like BDF1/2 show much more dissipation than explicit schemes.

Our second issue concerns an important complexity issue in unsteady mesh adaptation. Indeed, unsteady mesh adaptive calculations are penalized by the very small time-step imposed by accuracy requirements on regions involving small space-time scales. This small time step is for example an important computational penalty for mesh adaptive methods of AMR type¹. This is also the case for unsteady fixed-point mesh-adaptive methods as in².

In that latter method, the loss of efficiency is even more crucial when the anisotropic mesh is locally strongly stretched. In², this loss is evaluated as limiting the numerical convergence order for discontinuities to 8/5 instead of second-order convergence.

This limitation also applies to mesh adaptation by mesh motion. Our second practical example will concentrate on the computation of an isolated traveling discontinuity. The discontinuity needs to be followed by the mesh, preferably in a mesh-adaptive mode. Except if the adaptation works in a purely Lagrangian mode, an implicit scheme will smear the discontinuity of the solution. An explicit scheme will applied a costly very small time step on the whole computational domain.

In order to overcome these problems, the multirate time stepping approach represents an interesting alternative. A part of the computational domain is advanced in time with the small time-step imposed by accuracy and stability constraints. Another part is advanced with the larger time-step giving a good compromise between accuracy and efficiency.

Bruno: une page de biblio?

The development of multirate schemes was first limited to ODEs and their application restricted to a low number of special industrial problems. The first multirate method was due to the pioneering work of Rice³. In this work, a system of first-order ODEs made of a latent component (slow variation) and an active component (fast variation) was considered. Runge-Kutta type integration methods were developed, in which different integration steps (large for the latent component and small for the active component) were used and appropriate extrapolations were made for the latent components when the active components are integrated. Following this early work, many other developments have been conducted in the field of multirate schemes and ODEs^{3,4,5,6,7,8,9,10,11,12,13,14}. These multirate strategies usually combine classic numerical integration methods (Backward Differentiation Formulas, Adams methods, Runge-Kutta schemes, Rosenbrock-Wanner methods), in which a large integration step is used for the slow subsystem of EDOs and a smaller integration step is used for the fast subsystem, with extrapolation/interpolation algorithms for coupling active to latent parts and vice versa. In order to assess their stability and efficiency, these multirate methods were applied to (more or less large) systems of stiff ODEs, often derived from electric circuits problems. As an example, in⁹, a multirate 4-steps Rosenbrock-Wanner method was implemented to solve systems of 250 – 4000 ODEs

⁰Abbreviations: CFD, Computational Fluid Dynamics

which model electric circuits, leading to a gain in efficiency up to 2.8 compared to a classic 4-steps Runge-Kutta method.

Fewer and more recent multirate works were conducted in the field of PDEs and hyperbolic conservations law^{15,16,17,18,19,20}, and rare applications were performed in Computational Fluid Dynamics (CFD)^{20,19} for which we are interested. The first multirate work dealing with hyperbolic problems and applications in CFD was made by Löhner *et al.*²⁰. A domain-splitting method was developed in which the Euler equations are discretized by a second order explicit finite element scheme (Taylor-Galerkin method of Donea) on a domain splitted in several subregions of different grid resolution. For the time-integration of the equations, larger time steps are used in subregions of coarser mesh fineness leading to an increase in efficiency. One- and two-dimensional test-cases were considered : a shock tube problem, and supersonic inviscid flows around a circular cylinder and past a wedge. The results showed that the method can handle shocks and that a speedup of 2 between the multirate scheme and its single-rate counterpart can be reached.

Another work of interest, more recent, is the one of Constantinescu *et al.*¹⁵ which focuses on the development of multirate methods for the solution of one-dimensional scalar hyperbolic equations. They propose strategies that are based on an appropriate transition between subregions of different local stability conditions where a classic Runge-Kutta scheme is used, by introducing buffer regions, where an adapted Runge-Kutta method is employed. The proposed multirate partitioned Runge-Kutta scheme is second order accurate, conservative and nonlinear stable. For the case of the one-dimensional Burger equation, speedups up to 2.5 are obtained.

In the context of parallel computing, an interesting work on multirate methods is the recent one of Seny *et al.*¹⁹. This work focuses on the efficient parallel implementation of explicit multirate Runge-Kutta schemes in the framework of discontinuous Galerkin methods. The multirate Runge-Kutta scheme used is the approach proposed by Constantinescu¹⁵. In order to optimize the parallel efficiency of the multirate scheme, they propose a solution based on multi-constraint mesh partitioning. The objective is to ensure that the workload, for each stage of the multirate algorithm, is almost equally shared by each computer core i.e. the same number of elements are active on each core, while minimizing inter-processor communications. The METIS software is used for the mesh decomposition, and the parallel programming is performed with the Message Passing Interface. The efficiency of the parallel multirate strategy is evaluated on three test cases: the wind driven circulation in a square basin and the propagation of a tsunami wave using a shallow water model (two-dimensional), and the acoustic propagation in a turbofan engine intake using the linearized Euler equations (three-dimensional). It is shown that the multi-constraint partitioning strategy increases the efficiency of the parallel multirate scheme compared to the classic single-constraint partitioning.

Bruno: une page de biblio?

Many works have been published on multirate methods in the field of ODE, see for example^{3,4,5,6,7,8,9,10,11,12,13,14}, but fewer works were conducted on multirate time advancing schemes for the solution of PDE and hyperbolic conservation laws^{15,16,17,18,19,20}, and rare applications were performed in Computational Fluid Dynamics (CFD), for shock propagation in²⁰ and for shallow water computations in¹⁹. Therefore, there is still much work to do to provide viable multirate methods for CFD applications.

In this work, we propose a new multirate scheme based on control volume agglomeration which is at the same time very simple and well suited to a large class of finite volume approximations. The agglomeration produces macro-cells by grouping together several neighboring cells of the initial mesh. The method relies on a prediction step where large time steps are used with an evaluation of the fluxes performed on the macro-cells for the region of smallest cells, and on a correction step advancing solely the region of small cells, this time with a small time step.

We demonstrate the method in a numerical framework using a vertex centered approximation, the mixed finite volume/finite element formulation.

Target applications are three-dimensional unsteady flows modeled by the compressible Navier-Stokes equations equipped with turbulence models and discretized on unstructured possibly deformable meshes. The numerical illustration involves the two above examples.

The proposed algorithm is described in Section 2. Section 3 provides some motivations of this construction. Section 4 gives several examples of applications.

2 MULTIRATE TIME ADVANCING BY VOLUME AGGLOMERATION

2.1 Finite-Volume Navier-Stokes

The multirate time advancing scheme based on volume agglomeration is developed for the solution of the three-dimensional compressible Navier-Stokes equations. The main assumption is that the computational domain is split into computational finite volume cells such that cells intersect only by their boundaries and cover the whole computational domain. The discrete Navier-Stokes system is assembled by into a flux summation Ψ_i summing convective and diffusive fluxes evaluated at all the interfaces separating two cells. More precisely, the finite-volume spatial discretization combined with an explicit forward-Euler time-advancing writes for the Navier-Stokes equations possibly equipped with a $k - \varepsilon$ model:

$$vol_i w_i^{n+1} = vol_i w_i^n + \Delta t \Psi_i, \quad \forall i = 1, \dots, ncell,$$

where vol_i is the volume of $cell_i$, Δt the time step, and $w_i^n = (\rho_i^n, (\rho u)_i^n, (\rho v)_i^n, (\rho w)_i^n, E_i^n, (\rho k)_i^n, (\rho \varepsilon)_i^n)$ are as usually the density, moments, total energy, turbulent energy and turbulent dissipation at $cell_i$ and time level t^n , and $ncell$ the total number of cells in the mesh.

Given an explicit -conditionally stable- time advancing, we assume that we can define a maximal stable time step (*local time step*) $\Delta t_i, i = 1, \dots, ncell$ on each node. The stable local time step is classically defined by the combination of a viscous stability limit and an advective one according to the following formula:

$$\Delta t_i \leq \frac{CFL \times \Delta l_i^2}{\Delta l(\|\mathbf{u}_i\| + c_i) + 2\frac{\gamma}{\rho_i} \left(\frac{\mu_i}{Pr} + \frac{\mu_{t_i}}{Pr_t} \right)} \quad (1)$$

where Δl_i is a local characteristic mesh size, \mathbf{u}_i the local velocity, c_i the sound celerity, γ the ratio of specific heats, ρ_i the density, $\frac{\mu_i}{Pr} + \frac{\mu_{t_i}}{Pr_t}$ the sum of local viscosity to Prandtl ratio, laminar and turbulent, and CFL a parameter depending of the time advancing scheme, of the order of unity. Using the local time step Δt_i leads to a stable but not consistent time advancing.

A consistent and stable time advancing should use a *global/uniform time step* defined by:

$$\Delta t = \min_{1, ncell} \Delta t_i.$$

2.2 Inner and outer zones

We first define the inner zone and the outer zone, the coarse grid, and the construction of the fluxes on the coarse grid, ingredients on which our multirate time advancing scheme is based. For this splitting into two zones, the user is supposed to choose a (integer) *time step factor* $K > 1$.

- **Definition of the Inner and Outer zones :**

- We define the **outer zone** as the set of cells i for which the explicit scheme is stable for a time step $K\Delta t$

$$\Delta t_i \geq K\Delta t,$$

- the **inner zone** is the set of cells for which

$$\Delta t_i < K\Delta t.$$

- **Definition of the coarse grid :**

- **Objective :**

- * Advancement in time is performed with time step $K\Delta t$
- * Advancement in time preserves accuracy in the outer zone
- * Advancement in time is consistent in the inner zone

In the example given below, the accuracy of the initial scheme can be defined as a third-order spatial accuracy on smooth meshes, through the use of a MUSCL-type upwind-biased finite volume, combined with a fourth-order time accuracy through the use of the standard Runge-Kutta scheme, see²¹ for details.

- A **coarse grid** is defined on the inner zone by applying cell agglomeration in such a way that on each macro-cell, the maximal local stable time step is at least $K\Delta t$. Agglomeration consists in considering each cell and aggregating to it neighboring cells which are not yet aggregated to an other one (Figure 1). Agglomeration into macro-cell is re-iterated until macro-cells with maximal time step smaller then $K\Delta t$ have disappeared.
- **Time-advancing on the macro-cells :**
 - * We advance in time the chosen explicit scheme on the coarse grid with $K\Delta t$ as time step.

- **Construction of the flux on the coarse grid**

- The nodal fluxes Ψ_i are assembled on the fine cells (as usual)
- Fluxes are summed on the macro-cells I (inner zone) :

$$\Psi^I = \sum_{k \in I} \Psi_k \quad (2)$$

Remark 1: Stability can be further reinforced by adding a smoothing of the coarse flux (inner zone) :

$$\Psi^I = \left(\sum_{K \in \mathcal{V}(I)} \Psi^K \text{vol}^K \right) / \left(\sum_{K \in \mathcal{V}(I)} \text{vol}^K \right). \quad (3)$$

We did not need to apply this flux-smoothing. \square

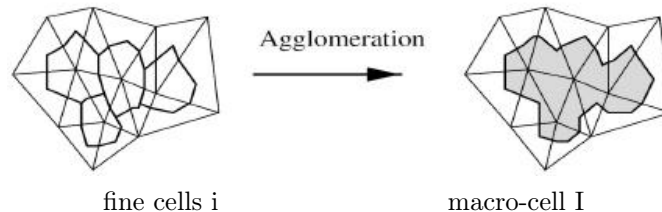


FIGURE 1 Sketch (in 2D) of the agglomeration of 4 cells into a macro-cell. Cells are dual cells of triangles, bounded by sections of triangle medians.

2.3 Multirate time advancing

The multirate algorithm is then based on a **prediction step** and a **correction step** as defined hereafter :

Step 1 (prediction step) :

The solution is advanced in time with time step $K\Delta t$, on the macro-cells in the inner zone and on the fine cells in the outer zone :

For $\alpha = 1, RKstep$

$$\text{outer zone : } \quad vol_i w_i^{(\alpha)} = vol_i w_i^{(0)} + b_\alpha K \Delta t \Psi_i^{(\alpha-1)} \quad (4)$$

$$\text{inner zone : } \quad vol^I w^{I,(\alpha)} = vol^I w^{I,(0)} + b_\alpha K \Delta t \Psi^{I,(\alpha-1)} \quad (5)$$

$$w_i^{(\alpha)} = w^{I,(\alpha)} \quad \text{for } i \in I \quad (6)$$

EndFor α .

where b_α denote the Runge-Kutta parameters, and vol^I the volume of macro-cell I .

Step 2 (correction step) :

- The unknowns are frozen in the outer zone at level $t^n + K \Delta t$.
- The outer unknowns near the boundary of the outer zone which are necessary for advancing the inner zone are interpolated in time.
- In the inner zone, using these interpolated values, the solution is advanced in time with the chosen explicit scheme and time step Δt .

This time advancing writes:

For $kt = 1, K$

For $\alpha = 1, RKstep$

$$\text{inner zone : } \quad vol_i w_i^{(\alpha)} = vol_i w_i^{(0)} + b_\alpha \Delta t \Psi_i^{(\alpha-1)} \quad (7)$$

EndFor α .

EndFor kt .

Remark 2: The complexity, proportional to the number of points in the inner zone, is therefore mastered. \square

3 ELEMENTS OF ANALYSIS

3.1 Stability

The central question concerning the coarse grid is the stability resulting from its use in the computation.

Considering (1), we expect that the viscous stability limit will improve by a factor four for a twice larger cell. The viscous stability limit can therefore be considered as more easily addressed by our coarsening. For the advective stability limit, we can be a little more precise. The coarse mesh is an unstructured partition of the domain in which cells are polyhedra. Analyses of time advancing schemes on unstructured meshes are available in L^2 norm for unstructured meshes, see^{22, 23, 24}. Here we solely propose a L^∞ analysis of the first order advection scheme. The gain in L^∞ stability can be analysed for a first-order upwind advection scheme. We get the following (obvious) lemma:

Lemma : The upwind advection scheme is positive on the mesh made of macro-cells as soon as for all macro-cell I :

$$\Delta t \|V_I\| < \left[\sum_{J \in \mathcal{N}(I)} \int_{\partial cell(I) \cap \partial cell(J)} d\Sigma \right]^{-1} \int_{cell(I)} dx$$

where $\mathcal{N}(I)$ holds for the neighbouring macro-cells of I . \square

The application of an adequate neighboring-cell agglomeration, producing large macro-cells of good aspect ration, combined with the smoothing effect of the mean applied on the residual will produce a K -times larger stability limit.

3.2 Accuracy

In contrast to more sophisticated multirate algorithms, the proposed method has not a rigorous control of the accuracy. Let us however remark that the generic situation involves variable-size meshes, which limits the unsteady accuracy on small scales propagation, already before applying the multirate method.

However the two following remarks tend to show that the scheme accuracy is conserved:

- the predictor step involves a sum of the fluxes and is at least as accurate as an equivalent coarse-grid approximation,
- assuming a reasonable mesh smoothness, the equivalent CFL on the inner part of the matching zone will be close to the explicit CFL applied on the outer part of the matching zone. Then the corrector step will improve the result in a way which depends on mesh smoothness, *i.e.* in better extent if the transition from small cells to larger cells is a smooth one.

In practice, most of our experiments will involve a comparison of explicit advancing and multirate advancing for the evaluation of a typical global output.

3.3 Efficiency

The proposed two-level multirate depends on only one parameter, the ratio K between the large and small time step. Considering a mesh with N vertices, a short loop on the mesh will produce the function $K \mapsto N^{small}(K) \leq N$ which gives the number of cells in the inner region for K .

If $CPU_{ExpNode}(\Delta t)$ denotes the CPU per node and per time step Δt of the underlying explicit scheme, a model for the multirate cpu per Δt would be

$$CPU_{MR(K)}(\Delta t) = \left(\frac{N}{K} + N^{small}(K) \right) \times CPU_{ExpNode}(\Delta t)$$

to be compared with the explicit case:

$$CPU_{Expli}(\Delta t) = N \times CPU_{ExpNode}(\Delta t).$$

We shall call the *expected gain* the ratio:

$$\text{Gain} = \frac{CPU_{Expli}(\Delta t)}{CPU_{MR(K)}(\Delta t)} = \frac{1}{\frac{1}{K} + \frac{N^{small}(K)}{N}}.$$

The above formula emphasizes the crucial influence of a very small proportion of inner cells.

Remark 3: In most other multirate methods, the phase with a larger time-step does not concern the inner region and then their gain would be modelled by:

$$\text{Gain} = \frac{1}{\frac{1}{KN}(N - N^{small}(K)) + \frac{N^{small}(K)}{N}}$$

Both gains are bounded by $N/N^{small}(K)$ and show that this ratio has to be sufficiently small. \square

Remark 4: Once we have evaluated $K \mapsto N^{small}(K)$ for a given mesh it is possible to predict a theoretical optimum K_{opt} for minimising the CPU time in scalar execution. However we shall see that the pertinence of the above theory will be strongly noised by implementation conditions. \square

3.4 Parallelism

The proposed method will be experimented with a parallel MPI software relying on mesh partitioning. The usual Metis software can be applied on the basis of a balanced repartition of the mesh. Then cell-agglomeration is applied at run time inside each partition, which saves communications.

However, as remarked in previous works (see for example¹⁹), if the mesh partition does not take into account the inner zone, then the work effort will not be balanced during the corrector.

The bad work balance for corrector can be of low impact if the corrector concerns a small enough part of the mesh, resulting in a small part of the global work.

But this is generally not the case. An option resulting from the work of Karypis and co-workers²⁵ and available in Metis is the application of a multi-constrained communication cost minimisation, with the two constraints that:

- partition is balanced for the whole computational domain, which will be favourable to the predictor phase,
- partition is balanced for the inner part of the computational domain, which will be favourable to the corrector phase.

Note that this partitioning algorithm produces a compromise between:

- the number of nodes in partitions of global mesh,
- the number of nodes in partitions of inner part of the mesh,
- the computational time in the multi-constrained communication of both partitions a model of which is minimised by the multi-constrained algorithm.

In some case, the user can specify a evident partition which perfectly balances the number of nodes in each partitions. In our experiments, we shall explicitly specify when it is the case and how it is performed.

4 APPLICATIONS

The multirate algorithm is implemented into the parallel (MPI) CFD code AIRONUM shared by INRIA, Lemma company and university of Montpellier. A description of this tool, which solves with a mixed element/volume method on unstructured meshes the compressible Euler and Navier-Stokes equations possibly equipped with a turbulence model, can be found in²⁶ and²⁷. The explicit time-advancing is a third-order Shu Runge-Kutta. The mean CPU for an explicit time step per mesh node is varying between 10^{-7} and 4×10^{-7} according to partition quality and number of nodes per subdomain. For some of the test cases, it will be interesting to compare the efficiency and accuracy of the proposed multirate time advancing with a implicit calculation of the same flow over the same interval. The implicit algorithm which we use combines a BDF2 time-approximation with a GMRES linear solver, using a Restrictive-Additive Schwarz préconditionner and ILU(0) in each partition, see²¹ for further details. In the cases computed with the implicit scheme, the CFL is fixed to 30 and the total number of GMRES iterations for one time step is around 20. For this CFL, the gain of an implicit computation with respect to an explicit one at CFL 0.5 is measured between 22. and 12. depending on the number of nodes per processor, the implicit scheme scalability being degraded with partitions less than 10,000 vertices while the explicit (and multirate) scheme remain scalable for partitions of 5,000 vertices. This BDF2 is of course second-order accurate in time and we shall use this property when estimating which timestep reduction is necessary for reducing by a given factor the deviation with respect to explicit time-advancing.

4.1 Contact discontinuity

In this first example, we consider the case of a moving contact discontinuity. For this purpose, the compressible Euler equations are solved in a rectangular parallelepiped as computational domain where the density is initially discontinuous at its middle (see Figure 2) while velocity and pressure are uniform.

The uniform velocity is a purely horizontal one. As can be seen in Figure 2, small cells are present on either side of the discontinuity. The mesh moves during the computation in such a way that the nodes located at the discontinuity are still the same, and that the number of small cells are equally balanced on either side of the discontinuity. An Arbitrary Lagrangian-Eulerian formulation is then used to solve the Euler equations on the resulting deforming mesh.

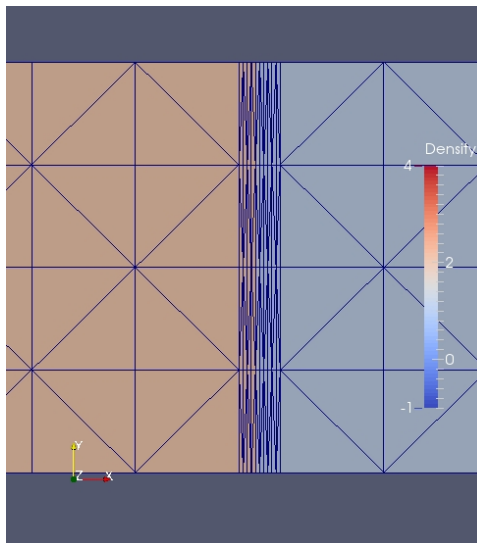


FIGURE 2 ALE calculation of a traveling contact discontinuity. Instantaneous mesh with mesh concentration in the middle of zoom and corresponding advected discontinuous fluid density.

K	$N^{small}(K)/N$ (%)	Expected gain (scalar)	CPU pred. phase (s/ $K\Delta t$)	CPU correc. phase (s/ $K\Delta t$)	Measured gain (parallel)
5	1.3	4.7	0.124	0.244	1.7
10	1.3	8.8	0.124	0.482	2.0
15	1.3	12.5	0.124	0.729	2.2

TABLE 1 ALE propagation of a contact discontinuity: Time step factor K , CPU of the explicit scheme per explicit time-step Δt and per node, percentage of nodes in the inner region, theoretical gain in scalar mode, CPU of the prediction phase per time-step $K\Delta t$, CPU of the correction phase per time-step $K\Delta t$, and measured parallel gain.

Our long term objective is to combine the multirate time advancing with a mesh adaptation algorithm in such a way that the small time steps imposed by the necessary good resolution of the discontinuity remain of weak impact on the global computational time.

The 3D mesh used in this simulation contains 25000 nodes and 96000 tetrahedra. The computational domain is decomposed into 2 subdomains, the partition interface being defined in such a way that it follows the center plan of the discontinuity.

When integer K , used for the definition of the inner and outer zones, is set to 5, 10 and 15, the percentage of nodes located in the inner zone is always 1.3%, which corresponds to the vertices of the small cells located on either side of the discontinuity. The CFL with respect to propagation is 0.5.

The multirate scheme with the aforementioned values of K , as well as a 4-stage Runge-Kutta method, are used for the computation. Each simulation was run on 2 cores of a Bullx B720 cluster. In Table 1, CPU times (prediction phase / correction phase) are given for the multirate approach and different time step factors K .

The correction phase, which consists of explicit time advancing on 1.3% of the mesh, concerns solely 78 vertices on each partition, 1.3% of the mesh, but finally the cpu cost appears as 38% of the cost on the whole partition. As a result, an improvement in the efficiency of about 1.7, 2.0 and 2.2 is observed when K is set to 5, 10 and 15, respectively, instead of the 4.7, 8.8 and 12.5 predicted by the theory.

K	$\frac{N^{small}}{N}$ (%)	Expected gain (theoretical)	CPU pred./corr. (s/ $K\Delta t$)	Measured gain (parallel)	Error (%)
10	0.015	8.69	1.81/4.36	2.93	$1 \cdot 10^{-5}$
40	0.04	15.38	1.83/17.3	3.82	$1.6 \cdot 10^{-4}$
BDF					
CFL=30				36.	$2 \cdot 10^{-2}$
CFL=2.7(est.)				3.29	$1.6 \cdot 10^{-4}$

TABLE 2 Spatial probe: Time step factor K , CPU of the explicit scheme per explicit time-step Δt and per node, percentage of nodes in the inner region, theoretical gain in scalar mode, CPU of the prediction phase per time-step $K\Delta t$, CPU of the correction phase per time-step $K\Delta t$, measured parallel gain, and relative error.

4.2 Spatial probe

We pass now to a less academic example, the supersonic flow around a probe model for Exomars (see for example²⁸). The Reynolds number is 1 million with respect to probe diameter. Delicate features in this simulation are a separation arising on a highly curved wall and relatively large recirculation zone at afterbody. Hybrid RANS-LES calculation brings more information than pure RANS does. The mesh involves 4,380,000 cells and the smallest mesh thickness is $2 \cdot 10^{-5}$. The smallest cells are only a few and are concentrated near the largest radius of the probe. For $K = 40$, their number is The mesh is partitioned with the usual option of Metis, into 192 subdomains.

A sketch of this flow is presented in Figure 4. The gain in efficiency varies from 2.93 with $K = 10$ and 657 cells in the inner zone to a maximum of 3.82 with $K = 40$ and 1752 cells in the inner zone (located in the high curvature region of the boundary layer where few very small cells are present). For $K = 40$, only 15 subdomains have inner cells with the usual partition. We observe that using the multirate approach instead of the explicit scheme produce a very low deviation of the lift history, compared to the implicit calculation (see Table 2 and Figure 3).

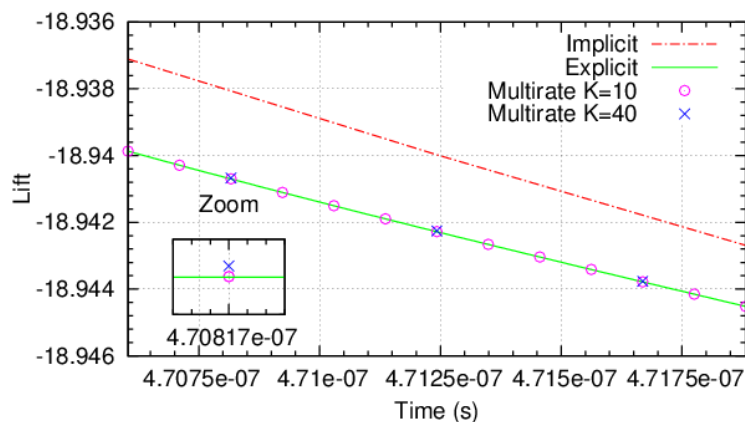


FIGURE 3 Spatial probe at Reynolds number 1 million. Zoom of the lift curves obtained with explicit, implicit and multirate schemes.

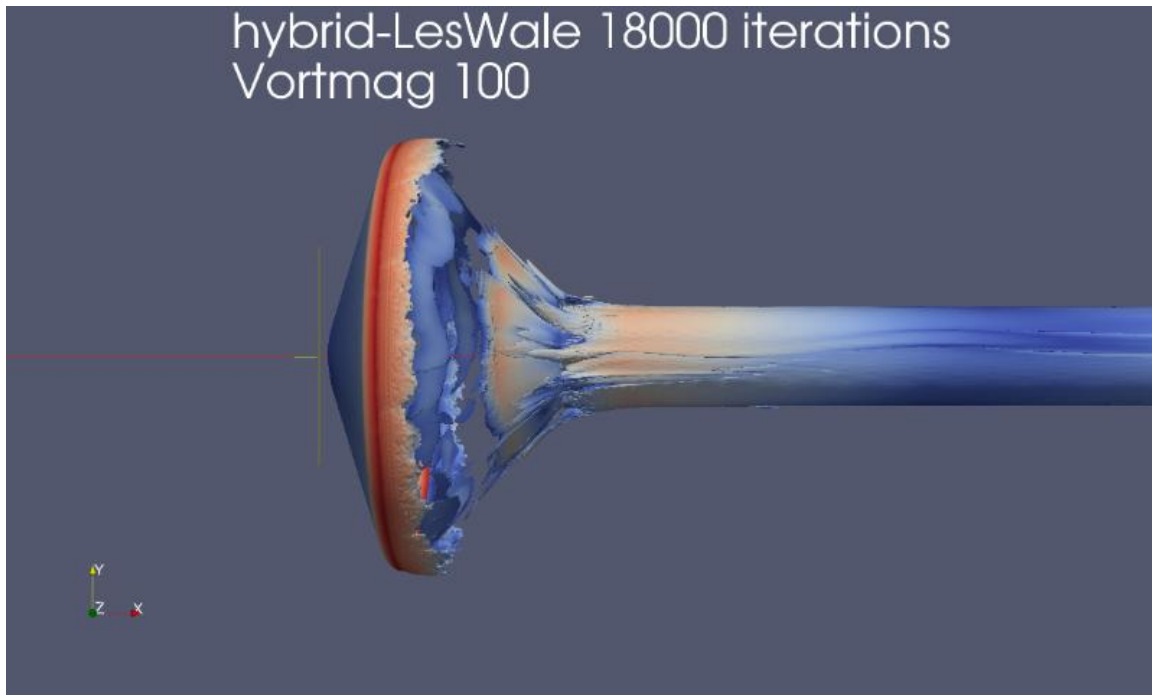


FIGURE 4 Spatial probe at Reynolds number 1 million. Q criterion.

4.3 Tandem cylinders

We turn now to a rather well-known benchmark test case, the calculation of a flow around a tandem cylinders at Reynolds number 1.66×10^5 . This was a test case of an AIAA workshop, see²⁹. It is a challenging computation since several complex flow features need to be captured around multiple bodies (stagnation zones, boundary layers, shear layers, separations, laminar-turbulent transition, recirculations, vortex sheddings, wakes). Furthermore, small cells are necessary for a proper prediction of the very thin boundary layers, which implies very small global time steps so that classical explicit calculations become very costly. The application of our multirate scheme to the tandem cylinders benchmark is also made more difficult by the fact that we use a hybrid turbulence model based on RANS and VMS-LES approaches²⁷, so that additional equations associated with turbulent variables need to be advanced in time.

In order to illustrate the quality of resolution, the Q-criterion isosurfaces are shown in Figure 5. It shows the complex flow features and the very small structures that need to be captured by the numerical model and the turbulence model, which renders this simulation particularly challenging. Further information concerning the comparison between computation and experiments are available in²⁷.

Two meshes were used for this study : a coarse mesh which contains 2.6 million nodes and 15 million tetrahedra, and a fine mesh with 16 million nodes and 96 million tetrahedra. For both meshes, the smallest cell thickness is $1.2 \cdot 10^{-4}$.

- **Coarse mesh**

The computational domain is decomposed into 192 subdomains. The CFL number is set to 0.5 for the explicit and multirate computations. When integer K , used for the definition of the inner and outer zones, is set to 2, 5 and 10, the percentage of nodes located in the inner zone is 4%, 16% and 25%, respectively (see Table 3).

CPU times (prediction phase / correction phase) are given in Table 3 for the multirate approach and different time step factors K . For this test case, the multirate scheme is not very efficient due to a too costly correction phase (a large number of inner nodes not equally distributed among the subdomains). It is true that the theoretical scalar gain is also rather small. One can notice that with an implicit simulation and a CFL number set to 30, the gain is 22 compared to the explicit option. However, the accuracy is degraded with the implicit

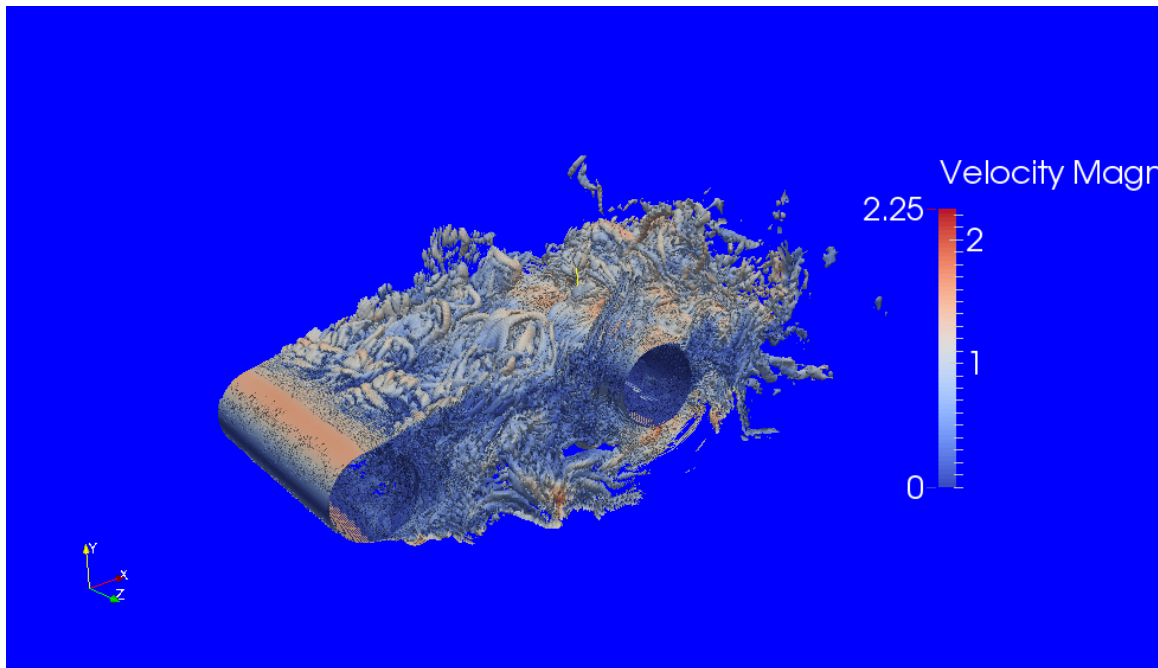


FIGURE 5 Tandem cylinders at Reynolds number 1.66×10^5 : instantaneous Q-criterion isosurfaces (coloured with velocity modulus).

approach (see the relative error in Table 3 and Figure 6).

K	$\frac{N^{small}}{N}$ (%)	Expected gain (scalar)	CPU(UP) pred./corr. (s/ $K\Delta t$)	Measured gain (UP/MCP)	Deviation(%) with explicit
2	4	1.85	0.92/0.86	1.03/-	$1.67 \cdot 10^{-5}$
5	16	2.77	0.92/4.10	0.92/-	$2.57 \cdot 10^{-5}$
10	25	2.86	0.92/8.48	0.98/-	$7.67 \cdot 10^{-4}$
20	30	-	-	1.2/1.29	$9 \cdot 10^{-4}$
BDF					
CFL=30				22./-	$2.5 \cdot 10^{-1}$
CFL=1.9(est.)				/-	$9 \cdot 10^{-4}$

TABLE 3 Tandem cylinder - coarse mesh (2.59 M nodes)- 192 processors.. Time step factor K , CPU of the explicit scheme per explicit time-step Δt and per node, percentage of nodes in the inner region, theoretical gain in scalar mode, CPU of the prediction phase per time-step $K\Delta t$, CPU of the correction phase per time-step $K\Delta t$, measured parallel gain, and relative error for the explicit, multirate and implicit BDF time advancing. UP holds for usual partition and MCP for multi-constrained partition.

- **Fine mesh:**

The computational domain is decomposed into 768 subdomains, and as many cores on a Bullx cluster were used to perform these computations. When integer K , used for the definition of the inner and outer zones, is set to 5, 10 and 20, the percentage of nodes located in the inner zone is 18%, 24% and 35%, respectively (see Table 4).

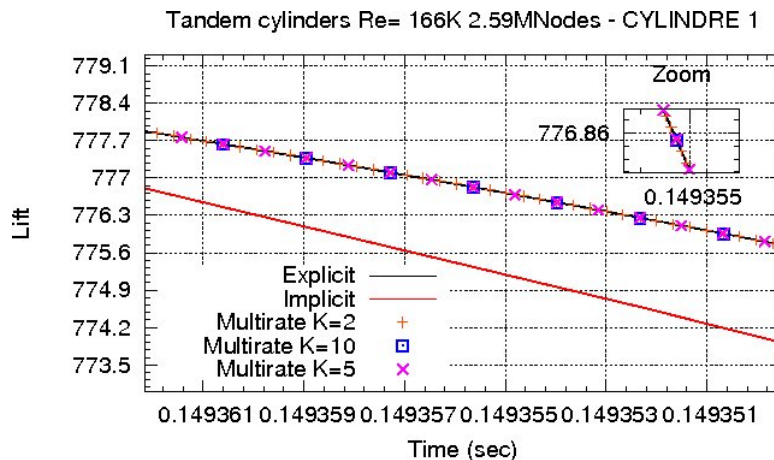


FIGURE 6 Tandem cylinder - coarse mesh (2.59 M nodes)- 192 processors. Zoom of the lift curves obtained with explicit, implicit and multirate schemes for the first cylinder.

K	$n_{proc.}$	$\frac{N^{small}}{N}$ (%)	Expected gain (scalar)	CPU(UP) pred./corr. (s/ $K\Delta t$)	Measured gain (UP/MCP)
5	768	18	2.63	1.55/6.9	0.91
10	768	24	2.94	1.52/14.1	0.99
20	768	35	2.50	1.53/28.9	1.02/2.0
20	192	35	2.50	-/-	-/1.77

TABLE 4 Tandem cylinder - fine mesh (16M nodes). Time step factor K , number of processors, CPU of the explicit scheme per explicit time-step Δt and per node, percentage of nodes in the inner region, theoretical gain in scalar mode, CPU of the prediction phase per time-step $K\Delta t$, CPU of the correction phase per time-step $K\Delta t$, and measured parallel gain. UP holds for usual partition and MCP for multi-constrained partition.

The CPU times for the explicit and multirate schemes are shown in Table 4. As for the coarse mesh and for the same reason, the multirate option turns out to be not very efficient. Again, the theoretical scalar gain is rather small in this case (see Table 4).

4.4 Circular cylinder at very high Reynolds number

The third application concerns the simulation of the flow around a circular cylinder at Reynolds number 8.4×10^6 . As for the previous benchmark, the computational domain is made of small cells around the body in order to allow a proper representation of the very thin boundary layer that occurs at such a high Reynolds number. On the other hand, the same hybrid RANS/VMS-LES model as that of the previous benchmark is used to compute this flow, which implies again that both the fluid and turbulent variables need to be advanced by the time integration scheme, and therefore also the multirate method. Figure 7 depicts the Q -criterion isosurfaces and shows the very small and complex structures that need to be captured by the numerical and the turbulence models, which renders this simulation very challenging.

The mesh used in this simulation contains 4.3 million nodes and 25 million tetrahedra. The smallest cell thickness is $2.5 \cdot 10^{-6}$. The computational domain is decomposed into 768 subdomains. When integer K , used for the definition of the inner and outer zones, is set to 5, 10 and 20, the percentage of nodes located in the inner zone is 15%, 19% and 24%, respectively (see Table 5).

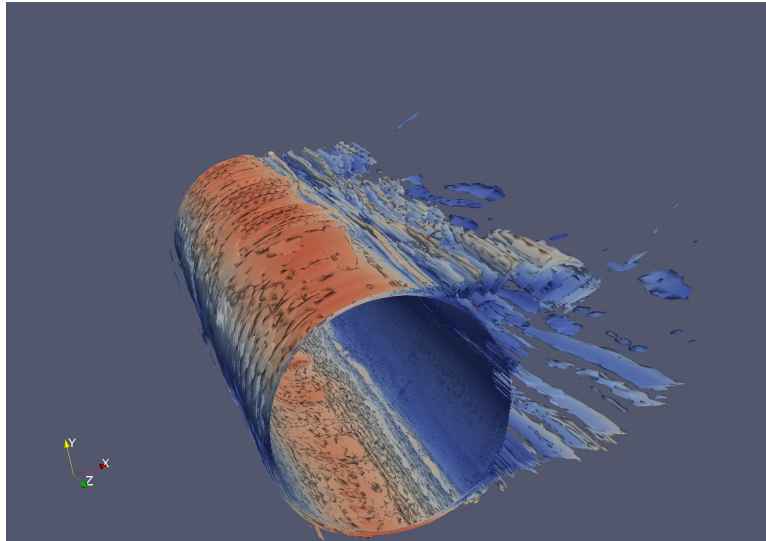


FIGURE 7 Circular cylinder at Reynolds number 8.4×10^6 . Instantaneous Q-criterion isosurfaces (coloured with velocity modulus).

K	$nproc$	$\frac{N^{small}}{N}$ (%)	Expected gain (scalar)	Measured gain (UP/MCP/R)	Error (%)
5	768	15	2.86	1.02/ - /-	$4.4 \cdot 10^{-4}$
10	768	19	3.45	1.11/ - /-	$7.8 \cdot 10^{-4}$
20	768	24	3.45	1.18/ - /-	$2.6 \cdot 10^{-3}$
20	384	24	3.45	1.18/1.51/-	$2.6 \cdot 10^{-3}$
20	192	24	3.45	-/1.43/2.27	$2.6 \cdot 10^{-3}$
60	192	27	3.48	-/1.52/2.32	$5 \cdot 10^{-3}$
BDF					
CFL=30	192			20./ - /-	1.0
CFL=2(est.)	192			1.5/ - /-	$5 \cdot 10^{-3}$
CFL=30	768			12.1/ - /-	1.0
CFL=2(est.)	768			0.9/ - /-	$5 \cdot 10^{-3}$

TABLE 5 Circular cylinder at Reynolds number 8.4×10^6 Time step factor K , CPU of the explicit scheme per explicit time-step Δt and per node, percentage of nodes in the inner region, theoretical gain in scalar mode, CPU of the prediction phase per time-step $K\Delta t$, CPU of the correction phase per time-step $K\Delta t$, measured parallel gain, and relative error for the explicit, multirate and implicit BDF time advancing. UP holds for usual partition, MCP for Metis multi-constrained partition, R for analytic radial optimal partition.

The explicit scheme is the 4-stage Runge-Kutta method. For each simulation, 768 cores were used on a Bullx B720 cluster, and the CFL number was set to 0.5. CPU times for the explicit and multirate schemes with different values of K are given in Table 5. One can observe that the efficiency of the multirate approach is rather moderate. The cost of the correction phase is indeed relatively high compared to the prediction phase. This is certainly due to an important number of inner nodes (which implies also a moderate theoretical scalar gain) and a non uniform distribution of these nodes among the computational cores. An implicit simulation, with a CFL number set to 30, was also performed. An important gain is observed compared to the multirate case, but at the cost of a degradation of the accuracy (see Table 5 and Figure 8) . In order to obtain the same level of error, the implicit time advancing, which is second-order

accurate in time, should be run with a CFL of 2, with a CPU time 10% larger (gain= 0.9) than for the explicit computation, or 2.57 times larger than with the $k = 60$ multirate computation.

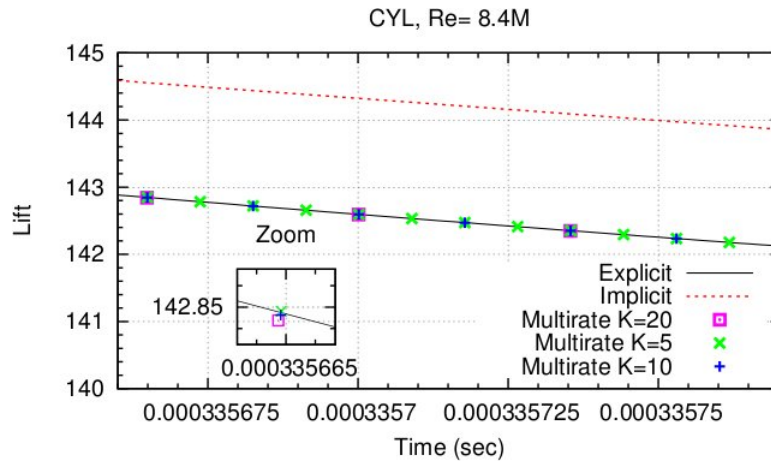


FIGURE 8 Circular cylinder at Reynolds number 8.4×10^6 . Zoom of the lift curves obtained with explicit, implicit and multirate schemes.

5 CONCLUSION

A new simplified multirate strategy for unstructured finite volume CFD is proposed in this work. The motivation of this research is two folds. First, the very high Reynolds number hybrid simulations can be computed with implicit time advancing for maintaining a reasonable cpu. But in many cases this is done with an important degradation of the accuracy with respect to smaller time steps on the same mesh. Second, with the arising of novel anisotropic mesh adaptation methods, the complexity of computations with large and small mesh sizes needs to be mastered with new methods. The proposed method is based on control volume agglomeration, and relies on:

- a prediction step where large time steps are used and where the fluxes for the smaller elements are evaluated on macro-cells for stability purpose,
- a correction step in which only the smaller elements of the so-called inner zone are advanced in time with a small time step.

The modification effort in an existing explicit unstructured code is very low.

Preliminary interesting results are given. They show that the proposed multirate strategy can be applied to complex unsteady CFD problems such as the prediction of three-dimensional flows around bluff bodies with an hybrid RANS/LES turbulence model.

Simulations, representative of problems that can be encountered in industrial applications, up to a Reynolds number as high as 8.4 million are performed. For the considered flow calculations, the fully explicit option is still usable but of high computational cost.

All the numerical experiments are parallel computed with MPI. This allows to identify the main difficulty in obtaining high computational gain, which is related with the paralle efficiency of the computations restricted to the inner zone.

We observed that the proposed multirate strategy offers a superior efficiency when the number of inner nodes, associated with very small cells in the mesh, is rather moderate. Thanks to the use of an explicit Runge-Kutta time advancing, the time accuracy of the multirate scheme remains high and the dissipation remains low, as compared with an implicit computation. Only very small time-scales are lost with respect to a pure explicit computation.

The case of a simplified mesh adaptive calculation is also studied. Due to its simplicity, the proposed method can be easily extended to several multirate layers corresponding to different time step stability regions in order to

separate, for example in the case of three layers, very small scales from intermediate ones, and intermediate scales from larger ones. In a first series of numerical experiments, CPU gains are obtained with a usual mesh partition. We also performed calculations using a particular partition constrained by the balancing of both global mesh and inner nodes submesh. Ideally, the workload should be equally shared for both Step1 (prediction phase) and Step2 (correction phase) of the multirate algorithm. However, we could not obtain such an ideal partition with our meshes. Further work on partitioning is probably necessary to get perfectly balanced workloads without too large communication times. In summary, the proposed multirate method is easy to program into a complex CFD code, is very stable in practice and the loss of accuracy with respect to an explicit scheme is very low, in contrast to implicit BDF2-based calculations, although we applied the implicit scheme with a CFL of 30, not much larger than with the multirate calculation (CFL= 10 for $K = 20$ in our simulations). Implicit accuracy is limited not only by the intrinsic scheme accuracy but also by the conditions required to achieve greater efficiency which involve a sufficiently large time-step and a short, parameter dependant, convergence of the linear solver performed in the time advancing step. In contrast, explicit and multirate computations are parameter safe, and the accuracy of the multirate method is optimal in regions complementary to the inner zone, that is, in our vortex shedding flow simulations, where it can be necessary to propagate accurately vortices, for example from the first cylinder to the second one in the case of the tandem cylinders.

ACKNOWLEDGMENTS

This work has been supported by French National Research Agency (ANR) through “Modèle numérique” program (projet MAIDESC n^o ANR-13-MONU-0010). This work was granted access to the HPC resources of CINES under the allocations 2017-A0022A05067 and 2017-A0022A06386 made by GENCI (Grand Equipement National de Calcul Intensif).

Conflict of interest

The authors declare no potential conflict of interests.

References

1. Berger M. J., Colella P.. Local adaptive mesh refinement for shock hydrodynamics. *J. Comput. Phys.*. 1989;82:64-84.
2. Belme A., Dervieux A., Alauzet F.. Time Accurate Anisotropic Goal-Oriented Mesh Adaptation for Unsteady Flows. *J. Comput. Phys.*. 2012;239:6323-6348.
3. Rice J. R.. Split Runge-Kutta Method for Simultaneous Equations. *Journal of Research of the National Bureau of Standards - B. Mathematics and Mathematical Physics*. 1960;64B(3).
4. Andrus J.F.. Numerical solution of systems of ordinary differential equations separated into subsystems. *SIAM J. Numerical Analysis*. 1979;16(4).
5. Gear C.W., Wells D.R.. Multirate linear multistep methods. *BIT*. 1984;:484-502.
6. Skelboe S.. Stability properties of backward differentiation multirate formulas. *Applied Numerical Mathematics*. 1989;5:151-160.
7. Sand J., Skelboe S.. Stability of backward Euler multirate methods and convergence of waveform relaxation. *BIT*. 1992;32:350-366.
8. Andrus J.F.. Stability of a multi-rate method for numerical integration of ODE'S. *Computers Math. Applic.*. 1993;25, No 2:3-14.

9. Günther M., Rentrop P.. Multirate ROW methods and latency of electric circuits. *Applied Numerical Mathematics*. 1993;13:83-102.
10. Engstler C., Lubich C.. MUR8: a multirate extension of the eight-order Dormer-Prince method. *Applied Numerical Mathematics*. 1997;25:185-192.
11. Engstler C., Lubich C.. Multirate Extrapolation Methods for Differential Equations with Different Time Scales. *Computing*. 1997;58:173-185.
12. Günther M., Kvaerno A., Rentrop P., Guelhan A., Klevanski J., Willems S.. Multirate partitioned Runge-Kutta methods. *BIT*. 1998;38(2):101-104.
13. Günther M., Kvaerno A., Rentrop P.. Multirate partitioned Runge-Kutta methods. *BIT*. 2001;41(3):504-514.
14. Savcenco V., Hundsdorfer W., Verwer J.G.. A multirate time stepping strategy for stiff ordinary differential equations. *BIT*. 2007;47:137-155.
15. Constantinescu E., Sandu A.. Multirate Timestepping Methods for Hyperbolic Conservation Laws. *J. sci. Comp.* 2007;33(3):239-278.
16. Sandu A., Constantinescu E.. Multirate Explicit Adams Methods for Time Integration of Conservation Laws. *J. Sci. Comp.* 2009;38:229-249.
17. Mugg P.R.. Construction and analysis of multi-rate partitioned Runge-Kutta methods. *Thesis, Naval Postgraduate School, Monterey, California, June 2012.* ;.
18. Kirby R.. On the convergence of high resolution methods with multiple time scales for hyperbolic laws. *Mathematics of Computation*. 2002;72(243):129-1250.
19. Seny B., Lambrechts J., Toulorge T., Legat V., Remacle J.-F.. An efficient parallel implementation of explicit multirate Runge-Kutta schemes for discontinuous Galerkin computations. *J. of Comp. Phys.* 2014;256:135-160.
20. Löhner R., Morgan K., Zienkiewicz O.C.. The use of domain splitting with an explicit hyperbolic solver. *Comput. Methods Appl. Mech. Engrg.* 1984;45:313-329.
21. Koobus B., Alauzet F., Dervieux A.. Some compressible numerical models for unstructured meshes. In: Magoulès F., ed. *CFD Handbook*, Boca Raton, London, New York, Washington: CRC Press 2011.
22. Angrand F., Dervieux A.. Some explicit triangular finite element schemes for the Euler equations. *Int. J. for Numer. Methods in Fluids*. 1984;4:749-764.
23. Giles M.B.. Stability analysis of a Galerkin/Runge-Kutta Navier-Stokes discretisation on unstructured tetrahedral grids. *Journal of Computational Physics*. 1997;132(2):201-214.
24. Giles M.B.. Energy stability analysis of multi-step methods on unstructured meshes. *CFDL Report 87-1, MIT Dept. of Aero. and Astro.* 1987;.
25. Karypis G., Kumar V.. A Fast and High Quality Multilevel Scheme for Partitioning Irregular Graphs. *SIAM J. Sci. Comput.* 2006;20(1):359-392.
26. Moussaed C., Salvetti M.V., Wornom S., Koobus B., Dervieux A.. Simulation of the flow past a circular cylinder in the supercritical regime by blending RANS and variational-multiscale LES models. *Journal of Fluids and Structures*. 2014;47:114-123.
27. Itam E., Wornom S., Koobus B., Sainte-Rose B., Dervieux A.. Simulation of multiple blunt-body flows with a hybrid variational multiscale model. *Conference on Modelling Fluid Flow (CMFF 15) The 16th International Conference on Fluid Flow Technologies Budapest, Hungary, September 1-4.* 2015;.

28. Guelhan A., Klevanski J., Willems S.. Experimental Study of the Dynamic Stability of the Exomars Capsule. *In: Proceedings of 7th European Symposium on Aerothermodynamics. ESA Communications. 7th European Symposium on Aerothermodynamics, 9.-12. Mai 2011, Brugge, Belgium.* 2011;.
29. Lockard D.. Summary of the Tandem Cylinder Solutions from the Benchmark Problems for Airframe Noise Computations-I. *Proceedings of Workshop AIAA-2011-35.* 2011;.

